

Simultaneous Coordinate Calibrations by Solving the AX=YB Problem without Correspondence*

Haiyuan Li¹, Qianli Ma², Tianmiao Wang¹ and Gregory Chirikjian^{2*}

Abstract— In image-guided system, relationships of hand-eye (X) and robot-world (Y) coordinates have to be calculated and simultaneous solution is useful in sensor calibration problem. Due to asynchrony of sensors timing, the correspondence between A and B is unknown. A probabilistic method is presented to solve the homogeneous matrix equations without a priori knowledge of the correspondence. Using Euclidean-Group invariants, an exact solution can be found. We illustrate the calculation in numeric simulation including various numbers of robot movements. The results show the efficiency and robustness of the proposed simultaneous method.

I. INTRODUCTION

Image-guided system has been widely used in robotics such as robot assisted surgery, (more examples). Sensors such as a camera, a laser scanner or an ultrasound probe are usually mounted on the distal end of a robotic manipulator. For a typical “hand-eye” system as described above, the relative transformation of the sensor with respect to the end-effector should be accurately calibrated, and it is often characterized as the well known $\mathbf{AX}=\mathbf{XB}$ problem. A variation of this problem is characterized as the $\mathbf{AX}=\mathbf{YB}$ problem, where both the hand-eye transformation and the pose of the robot base with respect to the world frame need to be calibrated. In a typical environment setup, the relationship among the sensor frame, robot frame and world frame is variant and the uncertainties exist. Therefore, simultaneous coordinate calibrations have to be determined frequently in order to enable the robots to respond to dynamic environments.

In the $\mathbf{AX}=\mathbf{YB}$ problem, A_s and B_s can be respectively obtained via different sensors. The data streams can be in an asynchronous fashion due to the different working frequencies of the sensors. The asynchrony causes a shift between the two streams of data which damages the correspondence between A_s and B_s . In this paper, a novel method is presented to solve for an X and Y without the need to know a priori knowledge of the correspondence between A_s and B_s .

The hand-eye calibration problem can be modeled as the $\mathbf{AX} = \mathbf{XB}$, where A and B are the homogeneous transformation matrices describing the relative motions of end-

*This work is partially supported by NSF Grant RI-Medium: #IIS-1162095

¹Haiyuan Li and Tianmiao Wang is with the School of Mechanical Engineering and Automation, Beihang University, Beijing 100191, China
lihaiyuan@buaa.edu.cn

²Qianli Ma and Gregory Chirikjian with the Department of Mechanical Engineering, Johns Hopkins University, Baltimore, MD 21218, USA
gregc@jhu.edu

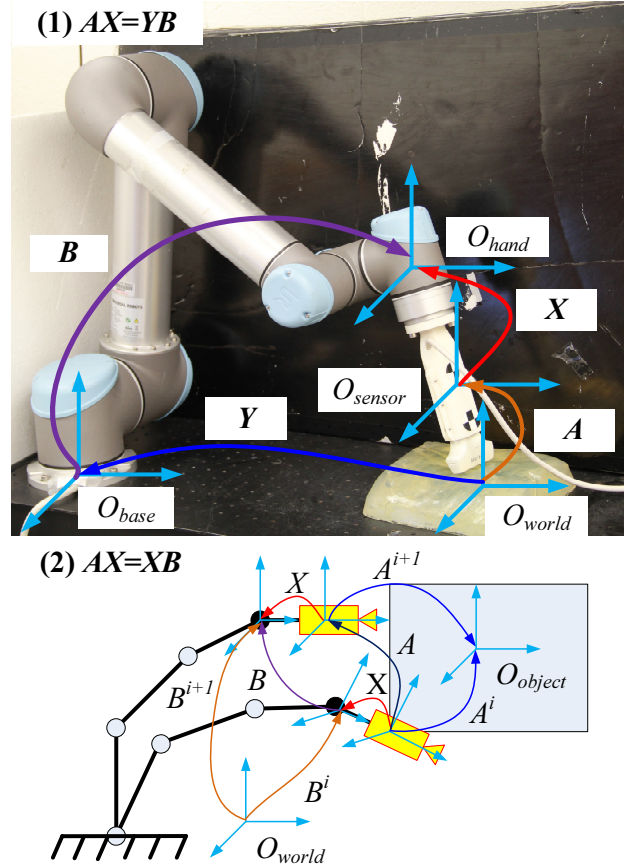


Fig. 1. (1) The hand-eye and robot-world calibration problem which is formulated as $\mathbf{AX}=\mathbf{YB}$ (The universal robot as shown in the picture is owned by professor Emad Boctor in). (2) The hand-eye calibration problem which is formulated as $\mathbf{AX}=\mathbf{XB}$.

effector and the sensor respectively. As shown in Fig. 1, $A = A^i(A^{i+1})^{-1}$ and $B = B^i(B^{i+1})^{-1}$. Given multiple pairs of $\{A, B\}$ with correspondence, many methods have been proposed to solve for X . To the best of the authors’ knowledge, Shiu [1] and Tsai [2] are the first to solve the $AX = XB$ sensor calibration problem. The other methods include but are not limited to the quaternion, dual quaternion, screw theory, Lie group theory convex optimization and gradient descent methods [3]–[9]. All of the methods above assume a prior knowledge of exact correspondence between A_i and B_i . For data streams $\{A_i\}$ and $\{B_i\}$ that are asynchronous, several methods have been proposed in the literature to solve for X using data without correspondence. These methods assume that there is exact knowledge of the A_s and B_s correspondence [10]–[12].

Simultaneous estimation of the hand-eye and robot-world transformations has been viewed as the $\mathbf{AX}=\mathbf{YB}$ problem. As shown in Fig. 1, Y is the transformation from the robot base to the world frame, A denotes the pose of the sensor in the world frame and B is the transformation from the end-effector to its fixed base. The A and B in $\mathbf{AX}=\mathbf{YB}$ are different from those in $\mathbf{AX}=\mathbf{XB}$ where the former uses absolute transformations and the latter uses relative transformations. This problem has been solved by many different methods such as kronecker product, quaternion, dual quaternion, and nonlinear optimization methods [13]–[20]. Simultaneous calibration of X and Y can be problematic in that all the methods above assume exact correspondence between $\{A_i\}$ and $\{B_j\}$, which is not the case in the real world. Another similar problem involves the calibration of multiple robots in terms of hand-eye, tool-flange and robot-robot system, and it is formulated as the $\mathbf{AXB}=\mathbf{YCZ}$ problem [21]. Simultaneous solution for X and Y in $\mathbf{AX}=\mathbf{YB}$ problem is an challenging issue. In the above methods, the correspondence between A and B is known a priori. In this paper, we focus on the $\mathbf{AX}=\mathbf{YB}$ problem which does not require a priori knowledge of the correspondence of the data streams.

The rest of the paper is organized as follows. In Section II, a novel probabilistic method is presented to solve for X and Y . In Section III, an algorithm involving both correlation theorem and Euclidean group invariants is proposed to recover the correspondence between $\{A_i\}$ and $\{B_j\}$. The simulation results which deal with noisy data without correspondence are illustrated in Section IV. Finally, conclusions are drawn based on the numerical results and possible future works are pointed out.

II. SOLVING $\mathbf{AX}=\mathbf{YB}$ USING A PROBABILISTIC METHOD ON MOTION GROUPS

In this section, a brief introduction to the concepts of probability density function on the special Euclidian group $SE(3)$ is presented and the probabilistic representation of $AX = YB$ are derived.

Any rigid transformation matrix can be viewed as a group element of $SE(3)$:

$$H(R, t) = \begin{pmatrix} R & t \\ 0^T & 1 \end{pmatrix} \in SE(3) \quad (1)$$

where $SO(3)$ denotes the special orthogonal group, $t \in \mathbb{R}^3$ is translational vector and H is symbol for group element.

Given a large set of pairs $(A_i, B_i) \in SE(3) \times SE(3)$ where $i = 1, \dots, n$, the following equation is true if the correspondence is known as a priori:

$$A_i X = Y B_i. \quad (2)$$

For a matrix $H \in SE(3)$, a Dirac delta function $\delta(H)$ is defined to be finite only at the identity and zero elsewhere:

$$\delta(H) = \begin{cases} +\infty, & H = I \\ 0, & H \neq I \end{cases} \quad (3)$$

It also satisfies the identity constraint as:

$$\int_{SE(3)} \delta(H) dH = 1. \quad (4)$$

A shifted Dirac delta function can be defined as $\delta_A(H) = \delta(A^{-1}H)$. Given $K, H \in SE(3)$ and two well-defined functions $f_1, f_2 \in (L^1 \cap L^2)(SE(3))$, their convolution on $SE(3)$ is defined as:

$$(f_1 * f_2)(H) = \int_{SE(3)} f_1(K) f_2(K^{-1} \circ H) dK. \quad (5)$$

Employing the properties of δ function, it is straightforward to see that:

$$(f * \delta)(H) = \int_{SE(3)} f(K) \delta(K^{-1} \circ H) dK = f(H). \quad (6)$$

Therefore, for each A_i and B_i , the following equations can be obtained:

$$(\delta_{A_i} * \delta_X)(H) = \delta(A_i^{-1} H X^{-1}) \quad (7a)$$

$$(\delta_Y * \delta_{B_i})(H) = \delta(Y^{-1} H B_i^{-1}). \quad (7b)$$

Using Eq.(2), the above two equations can be combined into a single equation as:

$$(\delta_{A_i} * \delta_X)(H) = (\delta_Y * \delta_{B_i})(H) \quad (8)$$

Define the probability density function of $\{A_i\}$ and $\{B_i\}$ as:

$$f_A(H) = \frac{1}{n} \sum_{i=1}^n \delta(A_i^{-1} H) \quad (9a)$$

$$f_B(H) = \frac{1}{n} \sum_{i=1}^n \delta(B_i^{-1} H) \quad (9b)$$

Using the distributivity of convolution, Eq.(9) can be substituted into Eq.(8) to get:

$$(f_{A_i} * \delta_X)(g) = (\delta_Y * f_{B_i})(g) \quad (10)$$

For each of the data stream $\{A_i\}$ and $\{B_i\}$, small relative motions are calculated between consecutive reference frames. Take $\{A_i\}$ for example, one metric of the distance between A_i and A_{i+1} can be defined as:

$$d^2(A_i, A_{i+1}) = \| \Delta A \|_W^2 = \text{trace}[(\Delta A) W (\Delta A)^T] = \epsilon, \quad (11)$$

where $\Delta A = A_i - A_{i+1}$ and $0 < \epsilon \ll 1$

The convolution of two “highly focused” probability density functions have some interesting properties that can be used to solve for X . In particular, define the mean M and covariance Σ of a probability density function on $SE(3)$ as:

$$\int_{SE(3)} \log(M^{-1} H) f(H) dH = 0 \quad (12a)$$

$$\Sigma = \int_{SE(3)} \log^\vee(M^{-1} H) [\log^\vee(M^{-1} H)]^T f(H) dH \quad (12b)$$

Then the corresponding discrete version is:

$$\sum_{i=1}^n \log(M^{-1}H) = 0 \quad (13a)$$

$$\Sigma = \sum_{i=1}^n \log^\vee(M^{-1}H)[\log^\vee(M^{-1}H)]^T \quad (13b)$$

While the cloud of frames A_i is clustered around M_A , an iterative formula can be used for computing M_A [22].

$${}^{k+1}M_A = {}^kM_A \circ \exp\left[\frac{1}{n} \sum_{i=1}^n \log({}^kM_A^{-1} \circ A_i)\right] \quad (14)$$

An initial estimate of the iterative procedure can be ${}^0M_A = \frac{1}{n} \sum_{i=1}^n \log(A_i)$, then the process iterates until the cost function, $\|\sum_{i=1}^n \log(M_A^{-1}A_i)\|^2$ falls below a predefined threshold, where the cost function is minimized and the minimum defines M_A . A similar procedure is used for computing M_B .

The mean and covariance for the convolution $(f_1 * f_2)(g)$ of two highly focused functions, f_1 and f_2 can be computed as

$$M_{1*2} = M_1 M_2 \quad (15a)$$

$$\Sigma_{1*2} = Ad(M_2^{-1})\Sigma_1 Ad^T(M_2^{-1}) + \Sigma_2 \quad (15b)$$

where

$$Ad(g) = \begin{pmatrix} R & O \\ \hat{t}R & R \end{pmatrix}$$

Because X and Y is fixed, as for $\delta_X(g)$ and $\delta_Y(g)$, mean and covariance are $M_X = X$, $\Sigma_X = 0$ and $M_Y = Y$, $\Sigma_Y = 0$, respectively, therefore we can obtain

$$M_AX = YM_B \quad (16a)$$

$$Ad(X^{-1})\Sigma_A Ad^T(X^{-1}) = \Sigma_B \quad (16b)$$

From (16a), we can obtain

$$R_{M_A}R_X = R_YR_{M_B} \quad (17a)$$

$$R_{M_A}t_X + t_{M_A} = R_Yt_{M_B} + t_Y \quad (17b)$$

$\begin{pmatrix} \Sigma_{M_A}^1 & \Sigma_{M_B}^1 \\ \Sigma_{M_A}^3 & \Sigma_{M_A}^4 \end{pmatrix}$ and $\begin{pmatrix} \Sigma_{M_B}^1 & \Sigma_{M_B}^2 \\ \Sigma_{M_B}^3 & \Sigma_{M_B}^4 \end{pmatrix}$ can be decomposed into blocks as $\begin{pmatrix} R_X^T & -R_X^T t_X \\ 0 & 1 \end{pmatrix}$, then we can write the first two blocks of (16b) as follows,

$$\Sigma_{M_B}^1 = R_X^T \Sigma_{M_A}^1 R_X \quad (18a)$$

$$\Sigma_{M_B}^2 = R_X^T \Sigma_{M_A}^1 R_X (\widehat{R_X^T t_X}) + R_X^T \Sigma_{M_A}^2 R_X \quad (18b)$$

The first blocks (18a) is eigendecomposed with the same diagonal matrix due to matrix similarity $\Sigma_{M_A}^1 = Q_{M_A} \wedge Q_{M_A}^T$, $\Sigma_{M_B}^1 = Q_{M_B} \wedge Q_{M_B}^T$. Then,

$$\wedge = (Q_{M_A}^T R_X Q_{M_B}) \wedge (Q_{M_B}^T R_X^T Q_{M_A}) = P \wedge P^T \quad (19)$$

In $P = Q_{M_A}^T R_X Q_{M_B}$, Q_{M_A} and Q_{M_B} are constrained to be a rotation matrix and therefore $P \in \Omega \cup (-\Omega)$,

$$\Omega = \left(\begin{array}{cc} \begin{pmatrix} 1 & 0 & 0 \\ 0 & 1 & 0 \\ 0 & 0 & 1 \\ -1 & 0 & 0 \\ 0 & 1 & 0 \\ 0 & 0 & -1 \end{pmatrix}, & \begin{pmatrix} -1 & 0 & 0 \\ 0 & -1 & 0 \\ 0 & 0 & 1 \\ 1 & 0 & 0 \\ 0 & -1 & 0 \\ 0 & 0 & -1 \end{pmatrix} \\ \end{array} \right) \quad (20)$$

Therefore, there are eight possibilities of $R_X, R_X = Q_{M_A}PQ_{M_B}^T$. Then, from 18b, eight t_X corresponding to R_X can be directly found. Furthermore, eight candidate R_Y and t_Y can be found. At last, there are eight possibilities of solution $(X_i, Y_i), i = 1, \dots, 8$. where,

$$X_i = \begin{pmatrix} R_X & t_X \\ \mathbf{0}^T & \mathbf{1} \end{pmatrix}, \quad Y_i = \begin{pmatrix} R_Y & t_Y \\ \mathbf{0}^T & \mathbf{1} \end{pmatrix} \quad (21)$$

Based on the screw theory, it is known that a homogeneous transformation H can be written in the form with four parameters $(\theta, d, \mathbf{n}, \mathbf{p})$.

$$H = \begin{pmatrix} e^{\theta \hat{\mathbf{n}}} & (\mathbf{I}_3 - e^{\theta \hat{\mathbf{n}}})\mathbf{p} + d\mathbf{n} \\ \mathbf{0}^T & \mathbf{1} \end{pmatrix} \quad (22)$$

$AX = YB$ can be written as $AX = X(X^{-1}YB)$ and let $B' = X^{-1}YB$. In the form $AX = XB'$, there exit two Euclidean-Group invariant relationships for one of eight groups of $(A_i, B_i^k) (i = 1, \dots, n; k = 1, \dots, 8), B_i^k = X^{-1}YB_i$ as follows,

$$\theta_{A_i} = \theta_{B_i^k}, d_{A_i} = d_{B_i^k} \quad (23)$$

From among the four pairs (X_i, Y_i) , we can find a correct solution to minimize the absolute deviations,

$$(X, Y) = \underset{(X_i, Y_i)}{\operatorname{argmin}} \frac{1}{n} \sum_{i=1}^n (\|\theta_{A_i} - \theta_{B_i^k}\| + \|d_{A_i} - d_{B_i^k}\|) \quad (24)$$

III. SOLUTION WITH UNKNOWN CORRESPONDENCE OF A_i AND B_i^k

In most cases, the homogeneous transformations with As and Bs are given based on the data from different sensors. Due to asynchronous timing of the measurement transmissions, the correspondences between A_i and B_i^k is unknown. The advantage of the above probabilistic solution lies on that X and Y can be calculated even if without any a priori knowledge of the correspondence. However, there are still eight possible candidate results (X_i, Y_i) . Using Euclidean-Group invariants, it is straightforward to determine which pair is the correct one if the correspondence between A_i and B_i^k can be known.

The Discrete Fourier Transform (DFT) decomposes a time-domain signal into its constituent frequencies. The input is a finite list of equally spaced samples of a function. Given a discrete signal consisting of a sequence of N complex numbers x_0, x_1, \dots, x_{N-1} , the DFT is denoted by $X_\kappa = \mathcal{F}x_n$

$$X_\kappa = \sum_{n=0}^{N-1} x_n \cdot \exp\left(-i \frac{2\pi}{N} n \kappa\right) \quad (25)$$

The Inverse Discrete Fourier transform (IDFT) denoted by

$$x_n = \frac{1}{N} \sum_{n=0}^{N-1} X_\kappa \cdot \exp\left(i \frac{2\pi}{N} n \kappa\right) \quad (26)$$

The discrete convolution of two sequences f_n and g_n are defined

$$(f * g)(\tau) = \sum_{i=0}^N f(t_i)g(t_i - \tau) \quad (27)$$

In convolution theorem, the Fourier transform of a convolution is the product of the Fourier transforms, namely,

$$f * g = \mathcal{F}^{-1}[\mathcal{F}(f) \cdot \mathcal{F}(g)] \quad (28)$$

The correlation theorem indicates that the correlation function, $\text{Corr}(f, g)$, will have a large value at a shift vector if the two sequences f and g contain similar features. The correlation can be obtained based on the convolution theorem. The DFT of the correlation $\text{Corr}(f, g)$ is equal to the product of the DFT of a sequence f_n and the complex conjugate \mathcal{F}^* of the DFT of the other sequence g_n .

$$\text{Corr}(f, g) = f \star g = \mathcal{F}^{-1}[\mathcal{F}(f) \cdot (\mathcal{F}(g))^*] \quad (29)$$

Compared with the standard time-domain convolution algorithm, the complexity of the convolution by multiplication in the frequency domain is significantly reduced with the help of the convolution theorem and the fast Fourier transform (FFT).

There are two sequences θ_{A_i} and $\theta_{B_i^k}$ from each pair (A_i, B_i^k) . For homogeneous transformations from which the range of θ can vary, two sequences θ_{A_i} and $\theta_{B_i^k}$ can be first normalized.

$$\theta_1 = \frac{(\theta_{A_i} - \mu_{A_i})}{\sigma_{A_i}}, \theta_2 = \frac{(\theta_{B_i^k} - \mu_{B_i^k})}{\sigma_{B_i^k}} \quad (30)$$

where μ_{A_i} ($\mu_{B_i^k}$) is the average of θ_{A_i} ($\theta_{B_i^k}$) and σ_{A_i} ($\sigma_{B_i^k}$) is the standard deviation.

Here, the correlation function $\text{Corr}(\theta_1, \theta_2)$ is the function of the time sequence index (n) which describes the probability that these two sequences are separated by this particular unit. The location of the function maximum indicates the amount of shift, τ_{shift} , between the two sequence θ_{A_i} and $\theta_{B_i^k}$.

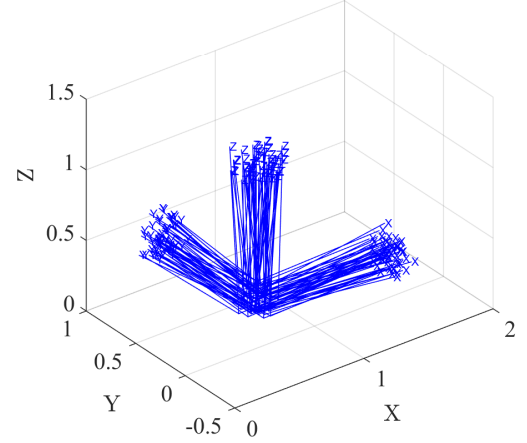


Fig. 2. B_s are randomly generated using $B_i = B_{init} \exp(\hat{x}), x = (x_1, \dots, x_6)^T, x_i \sim \mathcal{N}(0, 0.1)$.

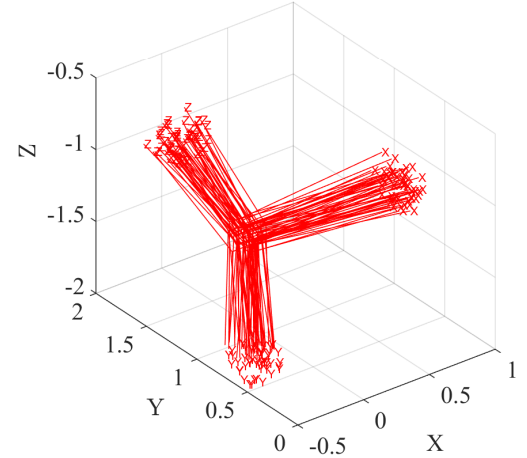


Fig. 3. A_s are calculated using $AX = YB$. X and Y are assumed.

$$\tau_{shift} = \underset{\text{index}}{\operatorname{argmax}}(\text{Corr}(\theta_1, \theta_2)) \quad (31)$$

Therefore, the correspondence between the two sequences can be found. The data of θ_{A_i} or d_{A_i} are shifted by $-\tau_{shift}$ to obtain a sequence of new pairs $(\theta_{A_i}(i + \tau_{shift}), \theta_{B_i^k})$ and $(d_{A_i}(i + \tau_{shift}), d_{B_i^k})$, $\max(i, i + \tau_{shift}) \leq i \leq \min(i, i + \tau_{shift})$. The data stream can be shifted to reach correspondence once the shift is found and the correct solution can also be found by minimizing the absolute deviations based on Euclidean-Group invariants relations using the method in Section II.

IV. SIMULATION STUDIES

In the numerical experiments in this section, the rotational and translational error for X and Y are measured as $\text{Error}(R_X) = \| \log^\vee(R_{X_{Solved}}^T R_{X_{true}}) \|$, $\text{Error}(t_X) = \| (t_{X_{Solved}} - t_{X_{true}}) \|$, $\text{Error}(R_Y) = \| \log^\vee(R_{Y_{Solved}}^T R_{Y_{true}}) \|$ and $\text{Error}(t_Y) = \| (t_{Y_{Solved}} - t_{Y_{true}}) \|$ respectively.

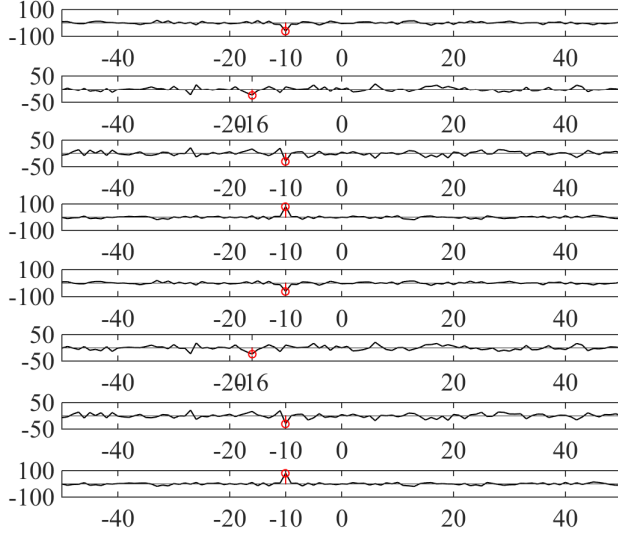


Fig. 4. The cross correlation of data streams of (A_i, B_i^k) respectively.

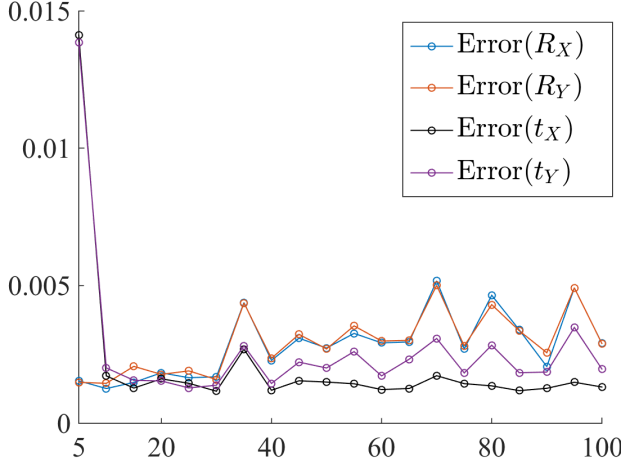


Fig. 5. Calculated rotational and translational deviation of X and Y solved using the data in Fig. 2 and Fig. 3.

B_i are generated randomly closely around B_{init} using $B_i = B_{init} \exp(\hat{\mathbf{x}})$ and i pose measurements were employed for generating i A_i by $A_i = Y B_i X^{-1}$ as shown in Fig. 2 in which a example shows A and B distribution. As a result by applying the above probabilistic method, 8 sequences $(\theta_{A_i}, \theta_{B_i^k})$ and $(d_{A_i}, d_{B_i^k})$ ($i = 5, \dots, 100, k = 1, \dots, 8$) can be obtained respectively.

If the data streams of As were shifted by m units compared to the data stream Bs . The maximum of cross correlation can be used to find the corresponding shift, which is $-m$ shown in Fig. 4, representing the data stream of B_i^k has been shifted by $-m$ units with respect to A_i . Therefore, we shift the data stream inversely to recover the correspondence for finding a correct solution satisfying Euclidean-Group invariants.

Using the minimum sum of $\|\theta_{A_i} - \theta_{B_i^k}\|$ and $\|d_{A_i} - d_{B_i^k}\|$,

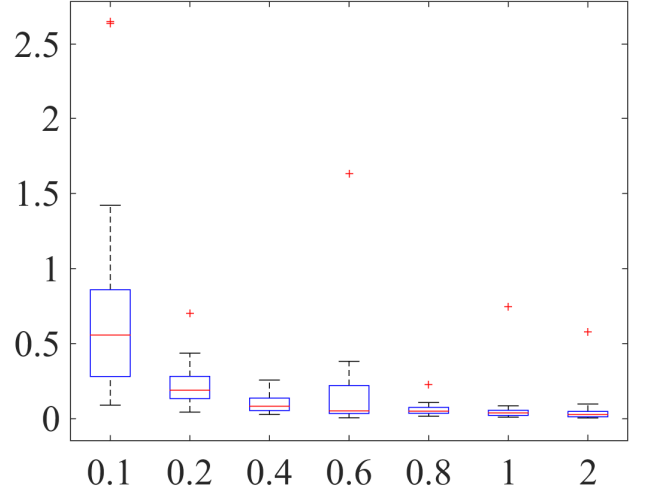


Fig. 6. $Error(R_X)$ distribution as the As and Bs spread ($\sigma(x_i) = 0.1, 0.2, 0.4, 0.6, 0.8, 1, 2$ as shown in Fig. 2)

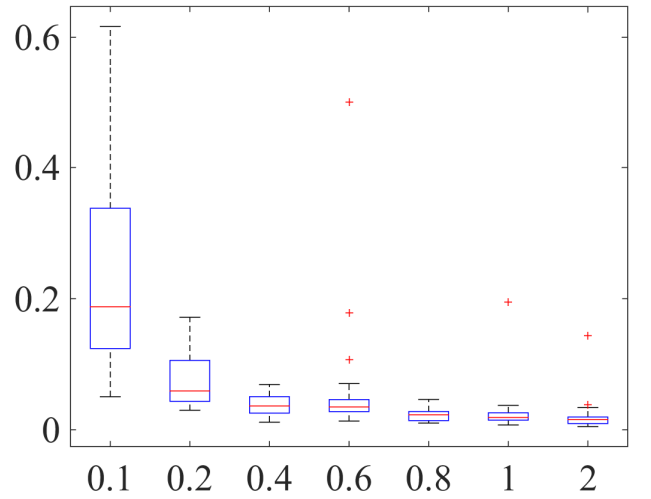


Fig. 7. $Error(R_Y)$ distribution as the As and Bs spread ($\sigma(x_i) = 0.1, 0.2, 0.4, 0.6, 0.8, 1, 2$ as shown in Fig. 2)

we can find the $B_i^k (k = 3)$ corresponding to the least sum of errors and then, only a (X_k, Y_k) is the desired solution. In Fig. 5, as the number of (A, B) pairs increase, the errors of translation and rotations are reduced but when the number comes to a certain value, the errors cannot be reduced furthermore.

In the generation of $B_i = B_{init} \exp(\hat{\mathbf{x}})$, each element x_j of $\mathbf{x} = (x_1, x_2, x_3, x_4, x_5, x_6)^T$ is Gaussian with $N \sim (\mu, \sigma)$. Small disturbances are exerted to the B_i to make the noisy $B_i^{noise} = B_i \exp(\hat{\mathbf{x}}_{noise})$, where each of Lie Algebra element of \mathbf{x} is Gaussian distribution $N \sim (\mu_{noise}, \sigma_{noise})$. In Fig. 8, 9, 10 and 11, σ_{noise} is 0.005. As σ varies from

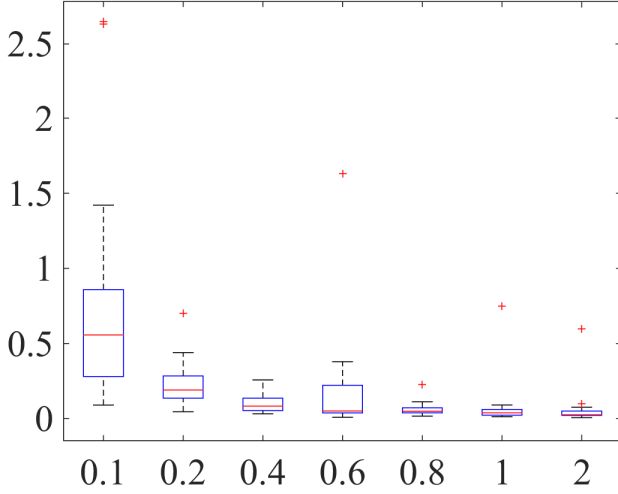


Fig. 8. $\text{Error}(t_X)$ distribution as the A s and B s spread ($\sigma(x_i) = 0.1, 0.2, 0.4, 0.6, 0.8, 1, 2$ as shown in Fig. 2)

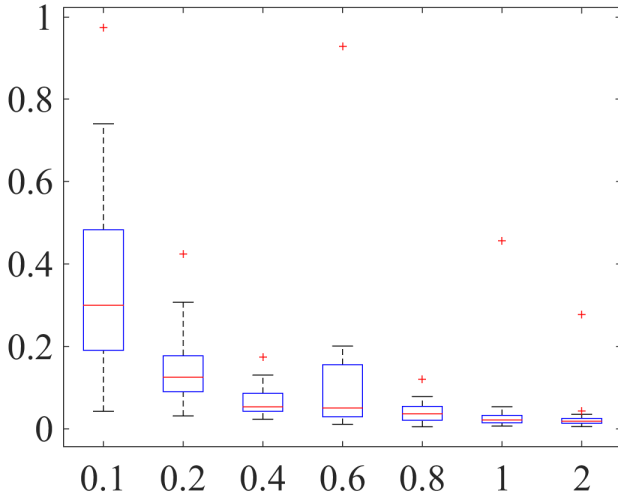


Fig. 9. $\text{Error}(t_Y)$ distribution as the A s and B s spread ($\sigma(x_i) = 0.1, 0.2, 0.4, 0.6, 0.8, 1, 2$ as shown in Fig. 2)

0.1 to 2, the errors of R_X , R_Y , t_X , and t_Y are reduced as shown in the box-and-whisker plot. There are several outliers not included between the whiskers. The median data can be used as the final solved X and Y .

V. CONCLUSIONS

In this paper, we developed a probabilistic approach to simultaneously obtain X and Y in $AX = YB$ sensor calibration problem. Without a prior knowledge of the correspondence between A and B , in the algorithm the probability theory in Lie group is used to constrain the solution of X and Y to eight candidates. As for the shifted data stream of A and B , using the correlation theorem with Euclidean group invariants, the correspondence is recovered to determine the correct solution from eight candidates. In

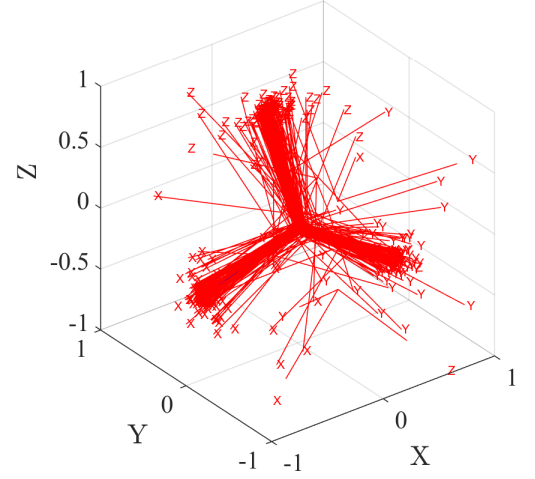


Fig. 10. The distribution of solved X .

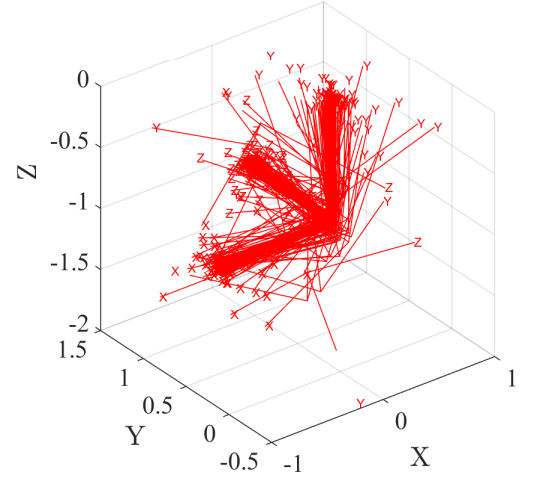


Fig. 11. The distribution of solved Y .

numeric simulation, the method perform well with different data samples.

APPENDIX ACKNOWLEDGMENT REFERENCES

- [1] Y. C. Shiu and S. Ahmad, "Calibration of wrist-mounted robotic sensors by solving homogeneous transform equations of the form $ax=xb$," *Robotics and Automation, IEEE Transactions on*, vol. 5, no. 1, pp. 16–29, 1989.
- [2] R. Y. Tsai and R. K. Lenz, "A new technique for fully autonomous and efficient 3d robotics hand/eye calibration," *Robotics and Automation, IEEE Transactions on*, vol. 5, no. 3, pp. 345–358, 1989.
- [3] C.-C. Wang, "Extrinsic calibration of a vision sensor mounted on a robot," *Robotics and Automation, IEEE Transactions on*, vol. 8, no. 2, pp. 161–175, 1992.
- [4] F. C. Park and B. J. Martin, "Robot sensor calibration: solving $ax=xb$ on the euclidean group," *IEEE Transactions on Robotics and Automation (Institute of Electrical and Electronics Engineers);(United States)*, vol. 10, no. 5, 1994.
- [5] R. Horaud and F. Dornaika, "Hand-eye calibration," *The international journal of robotics research*, vol. 14, no. 3, pp. 195–210, 1995.
- [6] K. Daniilidis, "Hand-eye calibration using dual quaternions," *The International Journal of Robotics Research*, vol. 18, no. 3, pp. 286–298, 1999.

- [7] I. Fassi and G. Legnani, "Hand to sensor calibration: A geometrical interpretation of the matrix equation $ax = xb$," *Journal of Robotic Systems*, vol. 22, no. 9, pp. 497–506, 2005.
- [8] Z. Zhao, "Hand-eye calibration using convex optimization," in *Robotics and Automation (ICRA), 2011 IEEE International Conference on*. IEEE, 2011, pp. 2947–2952.
- [9] M. K. Ackerman, A. Cheng, E. Boctor, and G. Chirikjian, "Online ultrasound sensor calibration using gradient descent on the euclidean group," in *Robotics and Automation (ICRA), 2014 IEEE International Conference on*. IEEE, 2014, pp. 4900–4905.
- [10] M. K. Ackerman and G. S. Chirikjian, "A probabilistic solution to the $ax = xb$ problem: Sensor calibration without correspondence," in *Geometric Science of Information*. Springer, 2013, pp. 693–701.
- [11] M. K. Ackerman, A. Cheng, B. Schiffman, E. Boctor, and G. Chirikjian, "Sensor calibration with unknown correspondence: Solving $ax = xb$ using euclidean-group invariants," in *Intelligent Robots and Systems (IROS), 2013 IEEE/RSJ International Conference on*. IEEE, 2013, pp. 1308–1313.
- [12] M. K. Ackerman, A. Cheng, and G. Chirikjian, "An information-theoretic approach to the correspondence-free $ax = xb$ sensor calibration problem," in *Robotics and Automation (ICRA), 2014 IEEE International Conference on*. IEEE, 2014, pp. 4893–4899.
- [13] H. Zhuang, Z. S. Roth, and R. Sudhakar, "Simultaneous robot/world and tool/flange calibration by solving homogeneous transformation equations of the form $ax = xb$," *Robotics and Automation, IEEE Transactions on*, vol. 10, no. 4, pp. 549–554, 1994.
- [14] F. Dornaika and R. Horaud, "Simultaneous robot-world and hand-eye calibration," *Robotics and Automation, IEEE Transactions on*, vol. 14, no. 4, pp. 617–622, 1998.
- [15] R. L. Hirsh, G. N. DeSouza, and A. C. Kak, "An iterative approach to the hand-eye and base-world calibration problem," in *Robotics and Automation, 2001. Proceedings 2001 ICRA. IEEE International Conference on*, vol. 3. IEEE, 2001, pp. 2171–2176.
- [16] F. Ernst, L. Richter, L. Matthäus, V. Martens, R. Bruder, A. Schlaefer, and A. Schweikard, "Non-orthogonal tool/flange and robot/world calibration," *The International Journal of Medical Robotics and Computer Assisted Surgery*, vol. 8, no. 4, pp. 407–420, 2012.
- [17] K. H. Strobl and G. Hirzinger, "Optimal hand-eye calibration," in *Intelligent Robots and Systems, 2006 IEEE/RSJ International Conference on*. IEEE, 2006, pp. 4647–4653.
- [18] A. Li, L. Wang, and D. Wu, "Simultaneous robot-world and hand-eye calibration using dual-quaternions and kronecker product," *Inter. J. Phys. Sci.*, vol. 5, no. 10, pp. 1530–1536, 2010.
- [19] M. Shah, "Solving the robot-world/hand-eye calibration problem using the kronecker product," *Journal of Mechanisms and Robotics*, vol. 5, no. 3, p. 031007, 2013.
- [20] J. Heller, D. Henrion, and T. Pajdla, "Hand-eye and robot-world calibration by global polynomial optimization," in *Robotics and Automation (ICRA), 2014 IEEE International Conference on*. IEEE, 2014, pp. 3157–3164.
- [21] J. Wang, L. Wu, M. Q.-H. Meng, and H. Ren, "Towards simultaneous coordinate calibrations for cooperative multiple robots," in *Intelligent Robots and Systems (IROS 2014), 2014 IEEE/RSJ International Conference on*. IEEE, 2014, pp. 410–415.
- [22] Y. Wang and G. S. Chirikjian, "Nonparametric second-order theory of error propagation on motion groups," *The International journal of robotics research*, vol. 27, no. 11-12, pp. 1258–1273, 2008.